RESEARCH ARTICLE

Intussusceptive lymphangiogenesis in the sinuses of developing human foetal lymph nodes

Lucio Díaz-Flores [a,*], Ricardo Gutiérrez [a], Mª Pino García [b], Miriam González-Gómez [a], Lucio Díaz-Flores Jr. [a], José Luis Carrasco [a]

[a] Department of Basic Medical Sciences, Faculty of Medicine, University of La Laguna, Tenerife, Spain
[b] Department of Pathology, Megalab, Tenerife, Spain

ARTICLE INFO

ABSTRACT

A meshwork of intraluminal processes in lymph node (LN) sinuses originates during LN development. Lymph flows through the meshwork, which has an important role in immunology and pathology. However, the formation mechanism of intraluminal processes has not been sufficiently studied. Our objective is to assess whether this mechanism is by intussusception, as occurs in transcapillary pillar formation in blood vessel intussusceptive angiogenesis. For this purpose, LNs with developing intrasinusal processes were used (human foetuses, 13–18 GW) for serial histologic sections and immunohistochemical procedures. The studies showed (a) sinuses originating from lymphatic sacs around expanded LN anlagen, (b) intra-sinus structures (lined by anti-podoplanin^{+}, VEGFR3^{+}, Prox-1^{+}, CD31^{+} lymphatic endothelial cells) with characteristics (in serial sections and 3D images) similar to those considered the hallmarks of intussusceptive angiogenesis, including pillars ($\leq$2.5 μm, with a collagen core), interstitial tissue structures (ITSs) or larger pillars (>2.5 μm, with a more cellular core) and folds (that form pillars when spanning), and (c) remodelled and fused pillars, ITSs and folds, which formed meshworks, compartmentalizing the sinuses into small intercommunicating spaces (segmentation). In conclusion, intussusception participates in the formation of the meshwork of processes in LN sinuses during LN development. This mechanism is also of interest because it contributes to the general knowledge of intussusceptive lymphangiogenesis (which has received less attention than intussusception in blood vessels), provides a basis for further studies and supports a new role for vessel intussusception (formation of an intraluminal meshwork with known action in fluid filtering, cell interactions and immunology).

© 2019 Elsevier GmbH. All rights reserved.

1. Introduction

Lymphatics are not required for the early steps of lymph node (LN) development (Vondenhoff et al., 2009a). However, they are critical for successive LN formation, maturation and functionality, as well as for the stabilization and maintenance of LN anlage stroma (Bénézech et al., 2010; Lee and Koh, 2016; van de Pavert and Mebius, 2014), which form a niche for lymphoid cells (Hoorweg et al., 2015). Thus, LNs and lymphatics develop within the same embryonic time frame and share several coordinated signals (Bénézech et al., 2010, 2014; Hoorweg et al., 2015; Lee and Koh, 2016; Onder et al., 2017; van de Pavert and Mebius, 2014; Vondenhoff et al., 2009a,b; Wang et al., 2018). Lymphatic

sprouts grow toward the LN anlage and form a lymphatic sac (Mebius, 2003) around the LN anlage, except in the mesenchymal hilus (Bailey and Weiss, 1975; Eikelenboom et al., 1978; Mebius, 2003; Willard-Mack, 2006). LN sinuses emerge from the lymphatic sac. A meshwork of intraluminal processes develops between the opposite walls of the sinuses (Moll et al., 2009). The mechanism of lymphangiogenesis that participates in the development of this intra-sinus meshwork has not been sufficiently studied. In lymphatic vessel remodelling during LN development, Bovay et al. (2018) described LN engulfment by lymphatic vasculature rather than by a sprouting response. In blood vasculature, the two principal types of growth and remodelling are sprouting and intussusceptive angiogenesis. The possibility of intussusceptive lymphangiogenesis, a non-sprouting intravascular process, in LN intra-sinus meshwork formation during development has not been explored.

Pillars/posts (diameter $\leq$2.5 μm), interstitial tissue structures (ITSs) or larger pillars (diameter >2.5 μm) and folds (that form pil-

lars when spanning) develop in intussusceptive angiogenesis (Burri and Tarek, 1990; Burri, 1990, 1992; Burri et al., 2004; Burri and Djonov, 2002; Díaz-Flores et al., 2017a,b; Djonov et al., 2000, 2002, 2003; Patan et al., 1992, 1993, 1996, 1997, 2001a,b, 2008). Vascular expansion and remodelling occur through this non-sprouting angiogenesis. Vessel segmentation by pillars and ITSs has also been demonstrated in different sized blood vessels (Díaz-Flores et al., 2018a; Patan et al., 2001a,b). One question is whether a similar intussusceptive mechanism may occur in the development of the meshworks of intraluminal processes in LN sinuses. Therefore, a study to assess whether intussusceptive hallmarks are present in developing LNs is not only of interest to explain the formation of intra-sinus LN meshworks of intraluminal processes, but to demonstrate intussusceptive lymphangiogenesis as a counterpart to blood vessel intussusceptive angiogenesis.

The aim of this work is therefore to assess whether intussusceptive lymphangiogenesis is the mechanism that participates in the formation of meshworks of processes (sinus-traversing strands) extending through the sinus lumen during human LN development. For this purpose, we explored whether the hallmarks of vascular intussusception (pillars, ITSs and folds) are present in the developing meshworks of processes in human LNs (from the formation of a lymphatic sac around the LN anlage to the development of meshworks of processes in human foetuses of 13–18 gestational weeks, GW). We also attempted to demonstrate an exponent of intussusceptive lymphangiogenesis (which has received less attention than intussusception in blood vessels), as a basis for further studies of this intussusceptive lymphangiogenic type in other conditions.

2. Materials and methods

2.1. Tissue samples

Developing LNs were studied from human foetuses received at the Pathology Service (University Hospital, Basic Medical Science Department of the University of La Laguna, Tenerife, Spain) for examination following miscarriage. The LNs studied (n: 22, 13–18 GW, 12 males and 10 females) were from mesenteric, pancreatic-duodenal, inguinal and popliteal regions. The LNs had no pathologic modifications and presented successive LN anlage enlargement and developing sinuses and processes in their lumen. Ethical approval for this study was obtained from the Ethics Committee of La Laguna University (CEIBA2018-0322).

2.2. Light microscopy

Twelve specimens were fixed in Bouin's fixative (with restricted antibody use) and another ten in paraformaldehyde. All specimens were embedded in paraffin and cut into 3 μm-thick serial sections. The sections were stained with Haematoxylin and Eosin (H&E) and Trichrome staining (Roche, Basel, Switzerland. Ref. 6521908001).

2.3. Immunohistochemistry

Histologic sections were attached to silanized slides. After pre-treatment for enhancement of labelling, the sections were blocked with 3% hydrogen peroxide and then incubated with primary antibodies (10–40 min). The primary antibodies (Dako, Glostrup, Denmark, except VEGFR3 -Abcam, Cambridge, UK) used in this study were podoplanin monoclonal mouse anti-human, clone D2-40 (dilution 1:50), catalog No. M3619; VEGFR3 polyclonal rabbit anti-human (dilution: 1:200) catalog No. ab 27278, CD31 monoclonal mouse anti-human, clone JC70A (dilution 1:50), catalog No. IR610; CD34 monoclonal mouse anti-human, clone QBEnd-10 (dilution 1:50), catalog No. IR632; α-smooth muscle actin (αSMA)

monoclonal mouse anti-human, clone 1A4 (dilution 1:50), catalog No. IR611; vimentin monoclonal mouse anti-human, clone V9 (dilution 1:50), catalog No. IR630; CD45 monoclonal mouse anti-human, clones 2B11 + PD7/26 (dilution 1:50), catalog No. IR751; and NCAM-1 (CD56) monoclonal mouse anti-human, clone 123C3 (dilution 1:50), catalog No. IR628. The immunoreaction was developed in a solution of diaminobenzidine and the sections were then briefly counterstained with haematoxylin, dehydrated in ethanol series, cleared in xylene and mounted in Eukitt®. Positive and negative controls were used.

For double immunostaining, podoplanin antibody (diaminobenzidine, DAB, as chromogen) and anti-CD34, anti-αSMA, anti-vimentin and anti-CD45 (aminoethylcarbazole, AEC, substrate-chromogen) were used, respectively. In serial sections, the sections were double-stained with anti-podoplanin and each of the aforementioned antibodies, respectively.

2.3.1. Immunofluorescence in confocal microscopy

For immunofluorescence, tissue sections were obtained as described above. For antigen retrieval, sections were deparaffinized and boiled for 20 min in sodium citrate buffer 10 mM (pH 6), rinsed in Trisbuffered saline (TBS, pH 7.6, 0.05 M), and incubated with the following primary antibodies diluted in TBS overnight in a humid chamber at room temperature: mouse monoclonal anti-podoplanin (clone D2-40), rabbit polyclonal anti-Prox1 (ab37128, 1/100) and rabbit polyclonal anti-collagen type I (1/100 dilution, code AB749 P, Millipore). For the double immunofluorescence staining, sections were incubated with a mixture of monoclonal and polyclonal primary antibodies (anti-podoplanin + anti-collagen type I and anti-podoplanin + anti-Prox 1). The next day, the slides were rinsed in TBS and incubated for 1 h at room temperature in the dark with the secondary biotinylated goat anti-rabbit IgG (H + L) (1:500, Code: 65–6140, Invitrogen, San Diego, CA, USA) and Alexa Fluor 488 goat antimouse IgG (H + L) antibody (1:500, Code: A11001, Invitrogen), followed by incubation with Streptavidin Cy3 conjugate (1:500, Code: SA1010, Invitrogen) for 1 h at room temperature in the dark. Nuclei were detected by DAPI staining (Chemicon International, Temecula, CA, USA). After washing in TBS, sections were exposed to a saturated solution of Sudan black B (Merck, Barcelona, Spain) for 20 min to block autofluorescence. They were rinsed in TBS and were then cover-slipped with DABCO (1%) and glycerol-PBS (1:1). Negative controls were performed in the absence of primary antibodies. Fluorescence immunosignals were obtained using a Fluoview 1000 laser scanning confocal imaging system (Olympus Optical).

3. Results

3.1. General characteristics of primitive LN sinuses

Primitive human LN sinuses were observed between 13–18 GW. Structures suggesting LN anlage were initially seen between a vein, with endothelial cells (ECs) stained with anti-CD34, and a lymphatic sac in a mesenteric LN, showing lymphatic endothelial cells (LECs) stained with anti-podoplanin (Fig. 1A). From GW 14 on, LN anlagen were expanded and the sinuses began to form in mesenteric and pancreatic-duodenal LNs (sinuses in inguinal and popliteal LNs were at a slightly more advanced stage). The expanded anlage apparently pushed the future sinus visceral layer (with floor LECs) against the opposite future sinus parietal layer (with ceiling LECs) (Fig. 1B). The formation of the LN capsule, pillars, ITSs, and folds begins simultaneously with sinus development (Fig. 1C–E, G and H). Thus, from GW 15 on, pillars, ITSs and folds, the hallmarks of intussusception, were present between the opposite walls (parietal and visceral walls) of the sinuses, irrespective
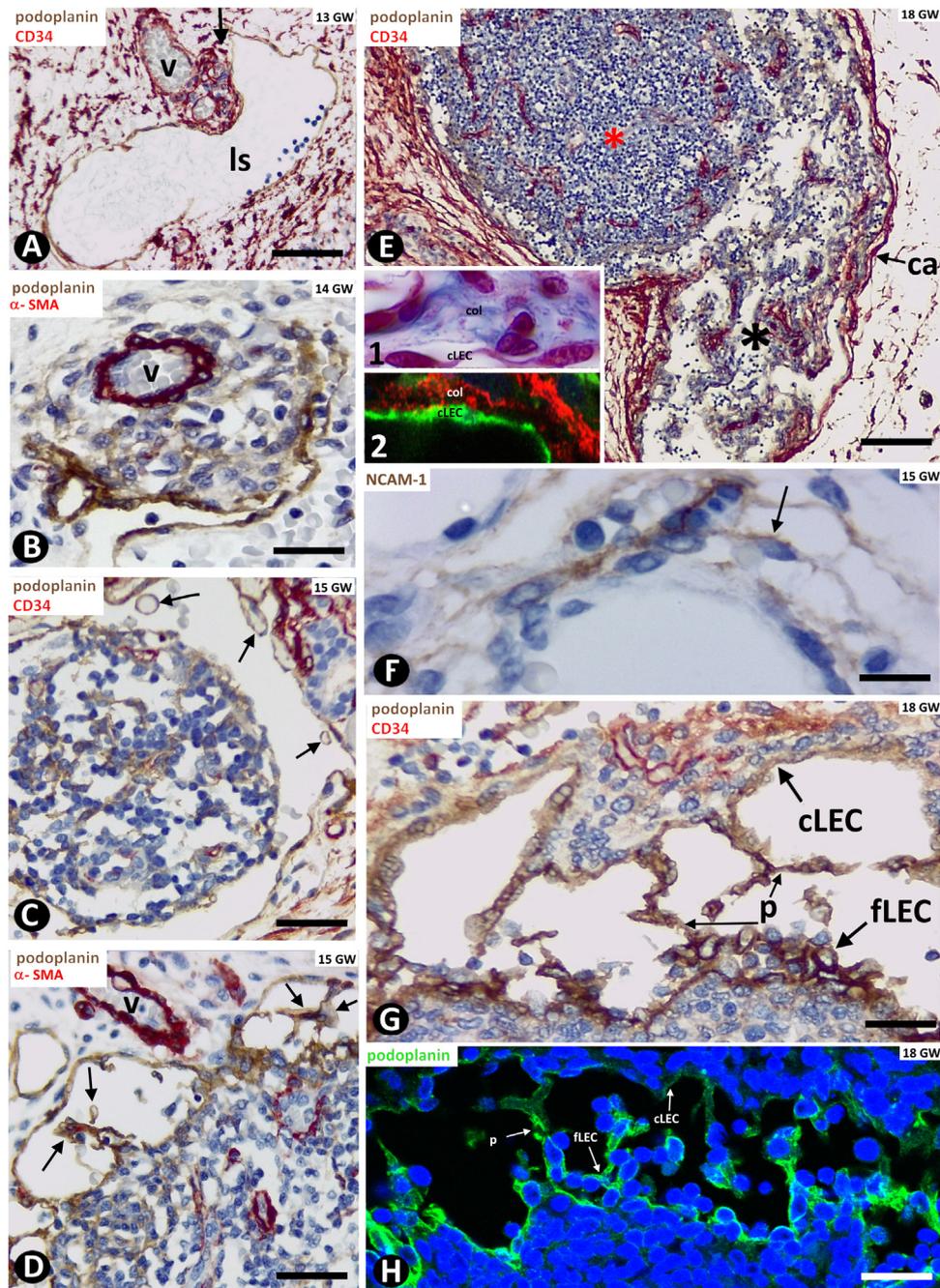
Fig. 1. Evolution of the lymphatic sacs around expanding LN anlagen is shown during lymph node development. Sections were double immuno-stained with anti-podoplanin (brown) and anti-CD34 (A, C, E and G) (red) and anti-αSMA (B and D) (red) and immunostained with NCAM-1 (F, brown) and podoplanin (H, confocal microscopy). A: Structure suggesting an LN anlage (arrow) with small blood vessels between a vein (v) (showing CD34+ endothelial cells) and a lymphatic sac (ls) (presenting anti-podoplanin+ LECs). Loose connective tissue is observed surrounding these structures (showing anti-CD34+ interstitial cells). B to D: Sinuses associated with expanded LN anlagen are seen in the space lined by anti-podoplanin+ LECs of the original lymphatic sac. Note some ITSs, pillars and folds formed in initial sinuses of the subcapsular zone (C, arrows) and of the primitive medulla around the hilum, in which a vein (v) is observed (with anti-αSMA+ cells) (D). E: Zones compatible with the LN cortex (red asterisk) (densely populated and with the subcapsular sinus) and with the LN primitive medulla (black asterisk) (predominance of ITSs). Note the LN capsule (ca) in which numerous anti-CD34+ interstitial cells form the external part, whereas Masson trichrome blue-stained collagen material (insert 1; col: collagen; cLEC: ceiling LECs) is prevalent in the internal part. Collagen I is demonstrated (insert 2: col: collagen I; cLEC: ceiling LECs; collagen I and podoplanin double-staining in confocal microscopy). F: NCAM-1+ (CD56) cells with thin processes in the LN capsule. G: CD34-positive interstitial cells in the capsule and subcapsular sinus with ceiling LECs (cLEC), floor LECs (fLEC) and pillars (p). Note that cLECs are flattened, while fLECs show more somatic cytoplasm and appear more stained by podoplanin than cLECs. H: The characteristics of podoplanin+ cLECs and fLECs are also observed in confocal microscopy. A to E: mesenteric LNs; F: LN of inguinal region; G and H: pancreatic-duodenal LNs. A: 13 GW; B: 14 GW; C, D and F: 15 GW; E, G and H: 18 GW. Bar: A: 35 μm; B, C and D: 25 μm; E: 180 μm; F: 15 μm; G and H: 20 μm. (For interpretation of the references to colour in this figure legend, the reader is referred to the web version of this article.)

of LN location (see below). Simultaneously, images suggesting a primitive LN cortex and medulla were seen (Fig. 1E) (these images resembled the cortical and medullar zones after cortico-medullar differentiation in the rat — Eikelenboom et al., 1978). The medulla

began to develop in the area of the sinus facing the hilum, where penetrating blood vessels were present (Fig. 1D). Numerous anti-CD34+ interstitial cells (Fig. 1E and G) were observed forming the external part of the developing LN capsule (in human LNs, these
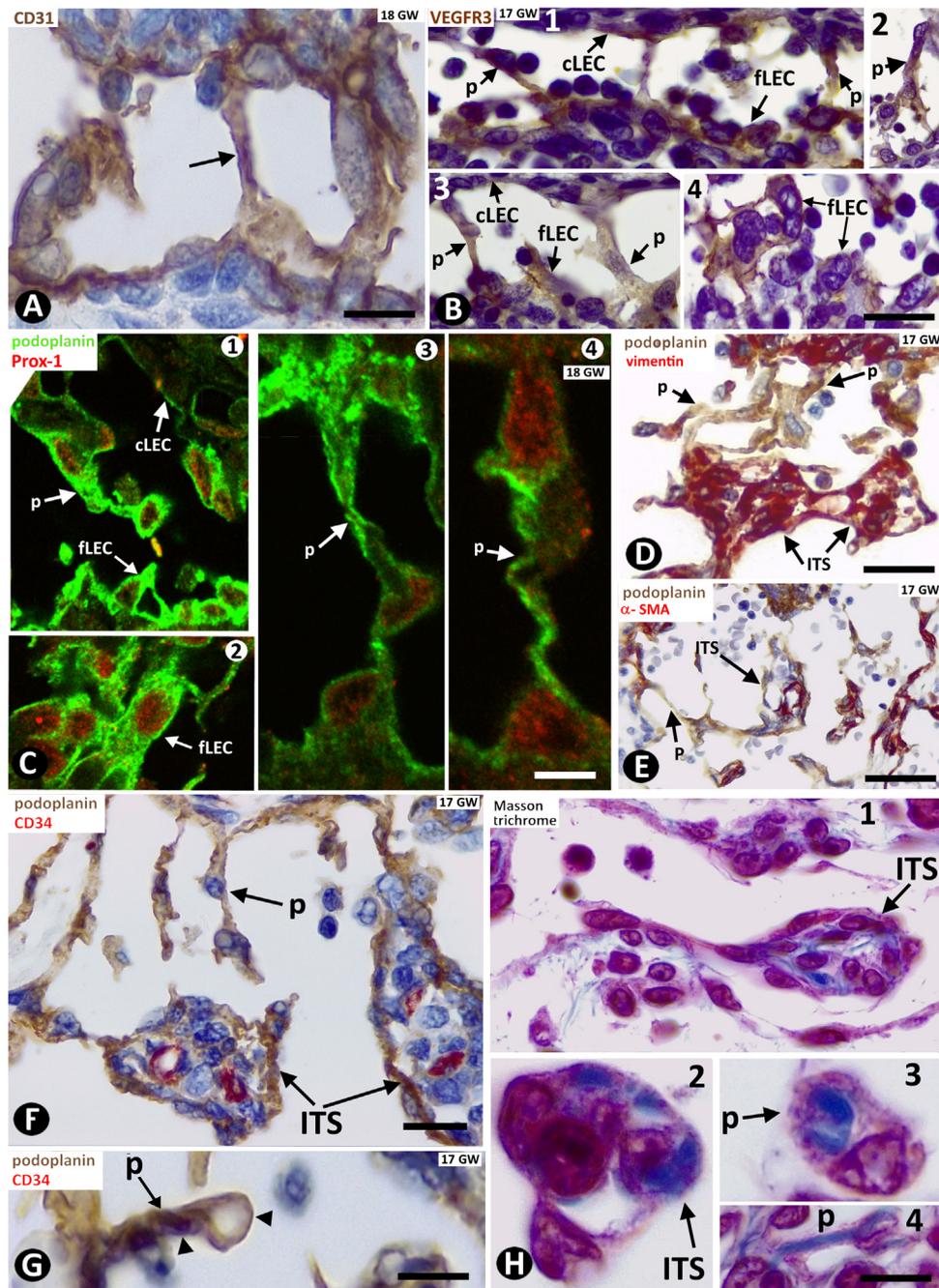
Fig. 2. Characteristics of ITSs and pillars in LN sinuses. Sections stained with anti-CD31, (brown) (A) and anti-VEGFR3 (brown) (B), double-immunostained with podoplanin (green) and Prox-1 (red) (C, in confocal microscopy), double-stained with anti-podoplanin (brown) and anti-vimentin (red) (D), anti-αSMA (red) (E) and anti-CD34 (red) (F and G), and stained with Masson Trichrome (H). A: LECs of the sinus and pillars (arrow) are observed expressing CD31. B (1, 2, 3 and 4): Expression of VEGFR3 in ceiling LECs (cLEC), floor LECs (fLEC) and LECs of pillars (p). C: Anti-podoplanin+ LECs, in pillars (p), cLECs and fLECs also show nuclear expression of Prox-1 in confocal microscopy. D-G: ITSs and pillars (p) covered by anti-podoplanin+ LECs are observed. In ITSs or larger pillars, the core is formed by anti-vimentin+ stromal cells (D), some anti-αSMA+ cells (E), small blood vessels (F) and collagen fibres (H, 1 and 2). In pillars with a smaller diameter, the core is generally only formed by packed collagen fibres (H, 3 and 4). Observe that pillars presented a transverse or longitudinal view depending on their irregular path (G, arrowheads). A-C: pancreatic-duodenal LNs; D-H: mesenteric LNs. A and C: 18 GW; B, D-H: 17 GW. Bar: A, C, F and G: 10 μm; B: 20 μm; D and E 25 μm; H1 and H4: 10 μm; H2 and H3: 2 μm. (For interpretation of the references to colour in this figure legend, the reader is referred to the web version of this article.)

cells could migrate from the adjacent vein adventitia, as occurs in murine LNs with the smooth muscle cells of the vein media layer — Bovay et al., 2018). Collagen material was mainly seen in the internal part of the capsule (Fig. 1E, insert 1). The presence of collagen I was demonstrated by confocal microscopy (Fig. 1E, insert 2). Some NCAM-1+ cells were also seen in the capsule (Fig. 1F). In advanced LN stages, differences were observed between ceiling or parietal LECs (with a flattened morphology and lower expression of the

podoplanin marker) and floor or visceral LECs (plumper and with a stronger expression of the podoplanin, CD31 and VEGFR3 markers) (Figs. 1G and H; 2 A and B). Several developing LNs were present in a single area, showing histologic variations, which mostly appeared to depend on the LN zone sectioned, rather than on different developmental stages.

The LECs of the LN sinuses expressed podoplanin (Fig. 1B–E, G and H), CD31 (Fig. 2A), VEGFR3 (Fig. 2B) and Prox-1 (Fig. 2C) (see

below), and the ECs of the blood vessels were positive for anti-CD34 (Fig. 1A) and anti-CD31. In veins, anti-αSMA$^+$ mural cells were also seen in their media layer (Fig. 1B and D).

3.2. Pillars, ITSs and folds in LN sinuses

Pillars, ITSs and folds, observed in the LNs studied, varied in size and showed a cover and a core (Figs. 1C–E, G and H; Fig. 2). In all these structures, the cover was formed by anti-podoplanin$^+$ (Figs.1C–E, G and H; Fig. 2D–G), anti-CD31$^+$ (Fig. 2A), anti-VEGFR3$^+$ (Fig. 2B) LECs. In confocal microscopy, anti-podoplanin$^+$ LECs, lining the sinuses, pillars, ITSs and folds, also presented nuclear expression of Prox-1 (Fig. 2C). In addition to variations in size, pillars and ITSs differed in core content. In pillars, with a diameter that ranged from 1 to 2.5 μm, the core contained packed collagen fibres (Figs. 2H,). In ITSs or larger pillars, with a diameter that generally ranged from 2.5 to 12 μm (exceptionally giant ITSs), the core was formed by anti-vimentin$^+$ stromal cells (Fig. 2D), some anti-αSMA$^+$ cells (Fig. 2E), small blood vessels (with ECs expressing CD34) (Fig. 2F) and collagen fibres (Fig. 2H, 1 and 2). Folds, which form pillars when spanning sinus walls, showed similar components (Figs. 1C, E and 2). In both pillars and ITSs, collagen was generally more condensed than in the LN capsule.

The number of pillars, ITSs and folds increased as the LN anlage expanded and the sinuses formed (Fig. 1). Depending on section and orientation, ITSs and pillars presented a transverse or longitudinal view (Fig. 2G), and appeared isolated or with zones connected to the sinus wall or to other ITSs and pillars (Fig. 2D–F). These connections were established by direct contact of the LECs lining ITSs, pillars and sinus walls (Fig. 3), or by LECs elongated between these structures (nascent pillars) (Fig. 3).

Most pillars and ITSs of the LN subcapsular sinus, covered by flattened LECs, showing an irregular path between the opposite walls of the sinus, appeared to originate from the sinus parietal layer and establish subsequent contact with prominent floor LECs. However, LECs of the ITSs and pillars in the areas closest to the visceral layer could also be more prominent, resembling sinusal floor cells (Fig. 1G and H). In the zones suggesting future medulla, the ITSs and their connecting pillars formed an intricate network with a smooth or varicose surface. Although both ITSs and pillars were observed in the medullary and subcapsular sinuses, ITSs were larger and more numerous (up to four times more) in the area suggesting the primitive medulla (Figs. 1E and 3) than in the subcapsular sinus (Fig. 4A–D).

Several morphologic findings related to the formation of pillars and ITSs were observed (see Section 4.3 of Discussion). These findings are as follows: (1) Contacts between the opposite LECs ("kissing contact" between ceiling and floor LECs) of the sinuses (Fig. 5A) and elongated LECs forming pillars (Figs. 2F, B) (pillar formation by "kissing contact"). (2) Bilayers of parietal LEC sheets penetrating the LN capsule and acquiring loop morphology (Fig. 5B). The internal LEC sheet layer of each loop surrounded a portion of the perisinusoidal tissue forming an ITS, whereas the external LEC sheet layer lined the connective tissue from which the ITS was segregated (Fig. 5C) (piecemeal form of ITS formation). Some ITS zones remained attached to the surrounding tissue, and blood vessels were observed passing through these connections (Fig. 5D). In pancreatic-duodenal LNs, fine nerve strands were occasionally incorporated into the ITS core (Fig. 5E). (3) Lymphatic vessels, whose walls contacted and merged, forming sinuses around anlagen (Fig. 5F and G). Pillars formed from these merged walls (Figs. 5G and H; 6 A and B) (pillar formation by "merging of adjacent capillaries") and vessel intercommunications were established through the spaces formed between the pillars and the remaining zones of the merged walls (Figs. 5G and H; 6 A and B). Projections of LECs

formed nascent pillars and connected the remaining walls, pillars and ITSs (Fig. 6B).

Appearance and disappearance of pillars and contact changes of ITSs were demonstrated in serial sections (Figs. 3 and 4), thereby confirming these structures as such. We also demonstrated these findings and 3D images of intussusceptive pillars at high magnification in confocal microscopy (Fig. 6C and D). In addition, the 3D images clearly showed a cover formed by podoplanin$^+$ LECs and the presence of collagen I in the core (Fig. 6D). Mitoses were not seen in LECs, which showed a minimal Ki-67 proliferative index (Fig. 6E–G).

3.3. Segmentation of LN sinuses by networks of ITSs and pillars

In the primitive subcapsular sinus, pillars, small ITSs and folds compartmentalized the sinus into numerous intercommunicating spaces, which increased the surface of lymph contact (Figs. 3 and 4). In the primitive medulla, lining LECs of the network of ITSs and of the ITS intercommunicating pillars (including nascent pillars) formed the coating of the medullary sinuses, whereas the core of these structures appeared to be the substrate of the medullary cords (Fig. 1E).

4. Discussion

We report (a) intussusceptive lymphangiogenesis in human LN sinuses during LN development (presence in the LN sinuses of pillars, ITSs and folds, which are the hallmarks of intussusception) and (b) participation of pillars, ITSs and folds in sinus segmentation with the formation of intercommunicating spaces in the subcapsular sinus and the sinuses and cords in the medulla. These issues are outlined below. In addition, we consider the possible mechanisms of pillar, ITS and fold formation.

4.1. Intussusceptive lymphangiogenesis in human LN sinuses during LN development

The bridges that form in the lumen of sinuses during LN development meet the characteristics of the pillars and ITSs described in intussusception in blood vessels (Burri and Tarek, 1990; Burri, 1992; Burri et al., 2004; Burri and Djonov, 2002; Díaz-Flores et al., 2017a,b; Djonov et al., 2000, 2002, 2003; Paku et al., 2011; Patan, 2001a,b; Ribatti and Djonov, 2012), blood vessel tumours and pseudo-tumours (Díaz-Flores et al., 2016, 2018b), and in dilated and segmented hemorrhoidal veins in hemorrhoidal disease (Díaz-Flores et al., 2018a). Indeed, these intrasinusal LEC-covered structures show a simple core formed by packed collagen fibres (pillars, with a diameter ≤2.5 μm) or a more complex core of collagen, interstitial cells and small blood vessels (ITSs or larger pillars, with a diameter >2.5 μm). Variations in the aspect of pillars and ITSs when viewed in tangential or longitudinal sections resulted from the irregular path of these structures.

The pillars described here also meet other important requirements for consideration as hallmarks of intussusception, including (a) their subsequent appearance and disappearance in serial sections (Patan et al., 2001a; De Spiegelaere et al., 2012), (b) three-dimensional demonstration (Burri and Tarek, 1990; Burri, 1992; Burri et al., 2004; Burri and Djonov, 2002; Díaz-Flores et al., 2017a,b; Djonov et al., 2000, 2002, 2003; Paku et al., 2011; Patan, 2001a,b) after reconstruction of serial images in confocal microscopy and (c) minimal LEC proliferation in the meshwork of pillars and ITSs, as occurs in intussusceptive angiogenesis in the endothelium that lines the pillars of blood vessels (Mentzer and Konerding, 2014).

Recently, some authors have indicated that lymphatic vessel expansion is different around the LN anlagen (where it occurs
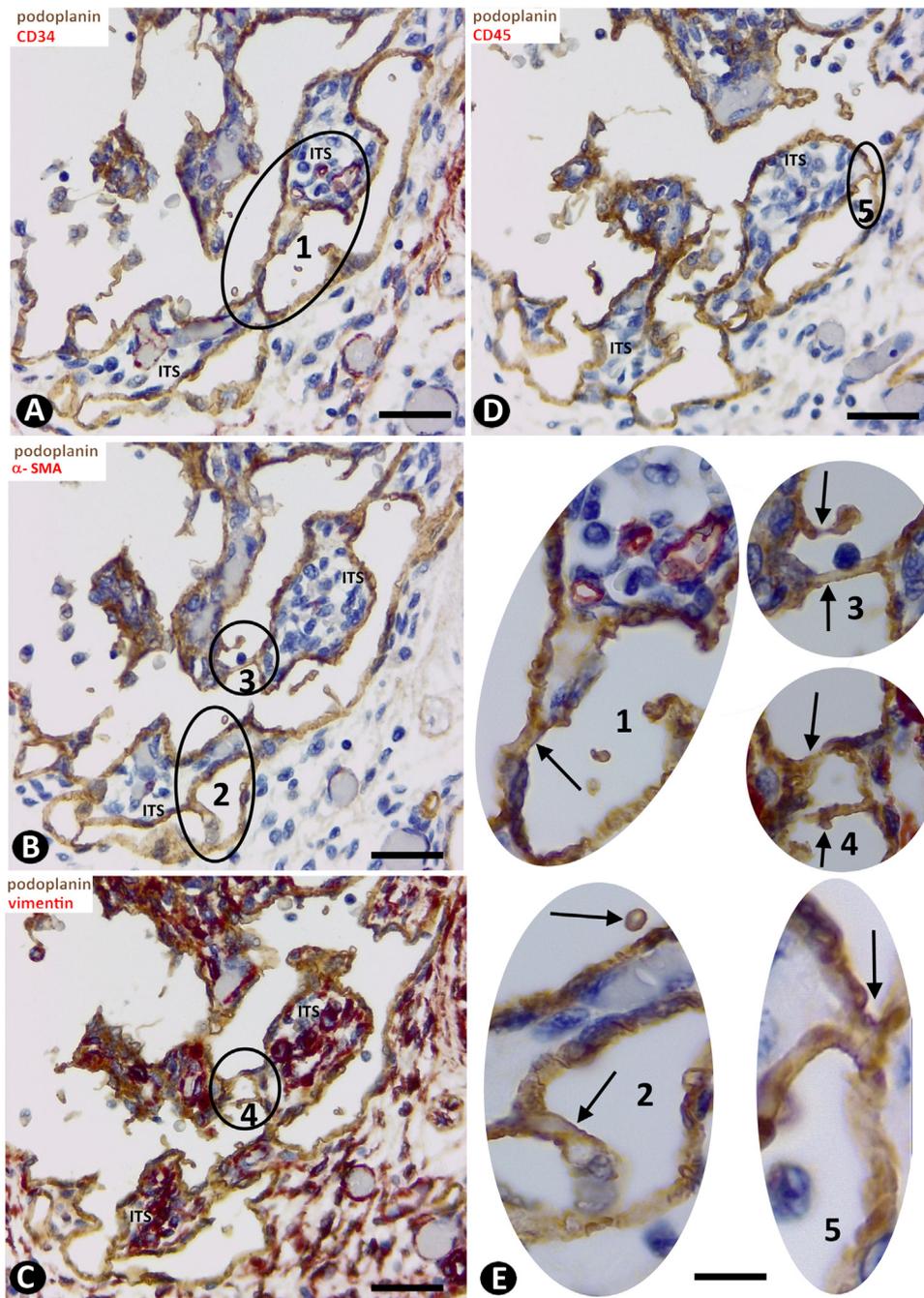
Fig. 3. Serial sections of a LN area showing large ITSs (whose size suggests that they belong to a peripheral zone of the primitive medulla), pillars and interconnecting LECs originating networks. Each of the serial sections is double-stained with anti-podoplanin (brown) and anti-CD34 (red) (A), anti-αSMA (red) (B), anti-vimentin (red) (C) and anti-CD45 (red) (D). Note the appearance and disappearance of pillars and the contact changes depending on the section. In the boxes, the pillars and LECs that participate in the ITS connections are observed under greater magnification. Note that these connections are established by extended pillars and LECs (1, 2, 3 and 4, arrows) or by direct contact of the lining LECs (5, arrow). In box 2, pillars appear longitudinally and transversally sectioned (arrows). A to E: mesenteric LNs. A to E: 17 GW. Bar: A to D: 25 μm; E: 10 μm. (For interpretation of the references to colour in this figure legend, the reader is referred to the web version of this article.)

by extension) than in other locations, such as skin lymphatics (where it occurs by sprouting). Indeed, the authors mainly describe a coordinated extension of continuous double LEC layers, which engulfed the LN anlagen and formed a double-walled surrounding cup-like structure, maintaining its integrity and function (Bovay et al., 2018). Our results concur with these observations on non-sprouting angiogenesis in LN sinuses and support intussusceptive rather than sprouting angiogenesis for intrasinusal bridge formation: presence of pillars and ITSs, with the aforementioned characteristics and requirements. These results and those observed in lymphatic pathology (including vascular trans-

formation of lymph node sinuses-Díaz-Flores et al., 2019, and lymphangiomas -non-published observation) can be a basis for further studies on lymphatic intussusception. Although pillars and ITSs appear to originate from the ceiling LECs of LN sinuses, participation of floor LECs is also possible.

4.2. Participation of pillars, ITSs and folds in sinus segmentation

Pillars, ITSs and folds can give rise to meshworks, which participate in blood vessel segmentation (Patan et al., 2001a,b; Díaz-Flores
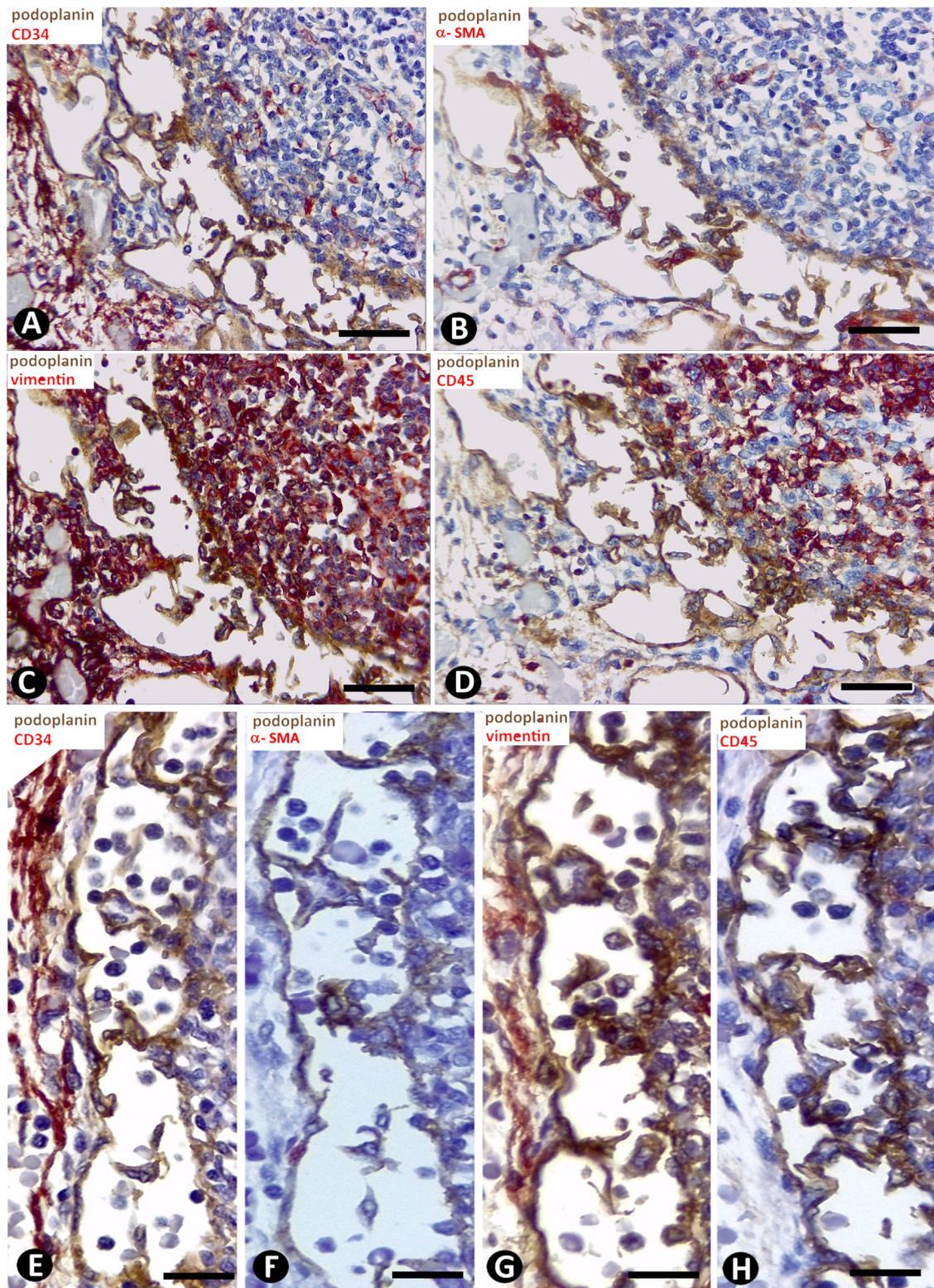
Fig. 4. Serial sections in a zone of the subcapsular sinus adjacent to the medulla (A to D) and in another subcapsular zone opposite the medulla (E to H). Sections are double-stained with anti-podoplanin (brown) and anti-CD34 (red) (A and E), anti-αSMA (red) (B and F), anti-vimentin (red) (C and G) and anti-CD45 (red) (D and H). Note that pillars and ITSs are present in the zone next to the medulla (A to D) and that pillars predominate in the cortical zone (E to H). The appearance and disappearance of the pillars and ITSs and their isolated or connected presentation in serial sections also depend on the section. A to H: mesenteric LNs. A to H: 17 GW. Bar: A to D: 25 µm; E to H: 15 µm. (For interpretation of the references to colour in this figure legend, the reader is referred to the web version of this article.)

et al., 2016, 2018b). In the primitive LN subcapsular sinus, abundant pillars and small ITSs can be the basis of the future meshwork formed by slim bridges, which compartmentalize the sinus into intercommunicating spaces. When cortico-medullary differentia-tion occurs, the zone where ITSs show a larger size, the ITS core and lining LECs (of ITSs and their interconnecting pillars) can form the substrate of future medullary cords and the sinus lining, respectively.
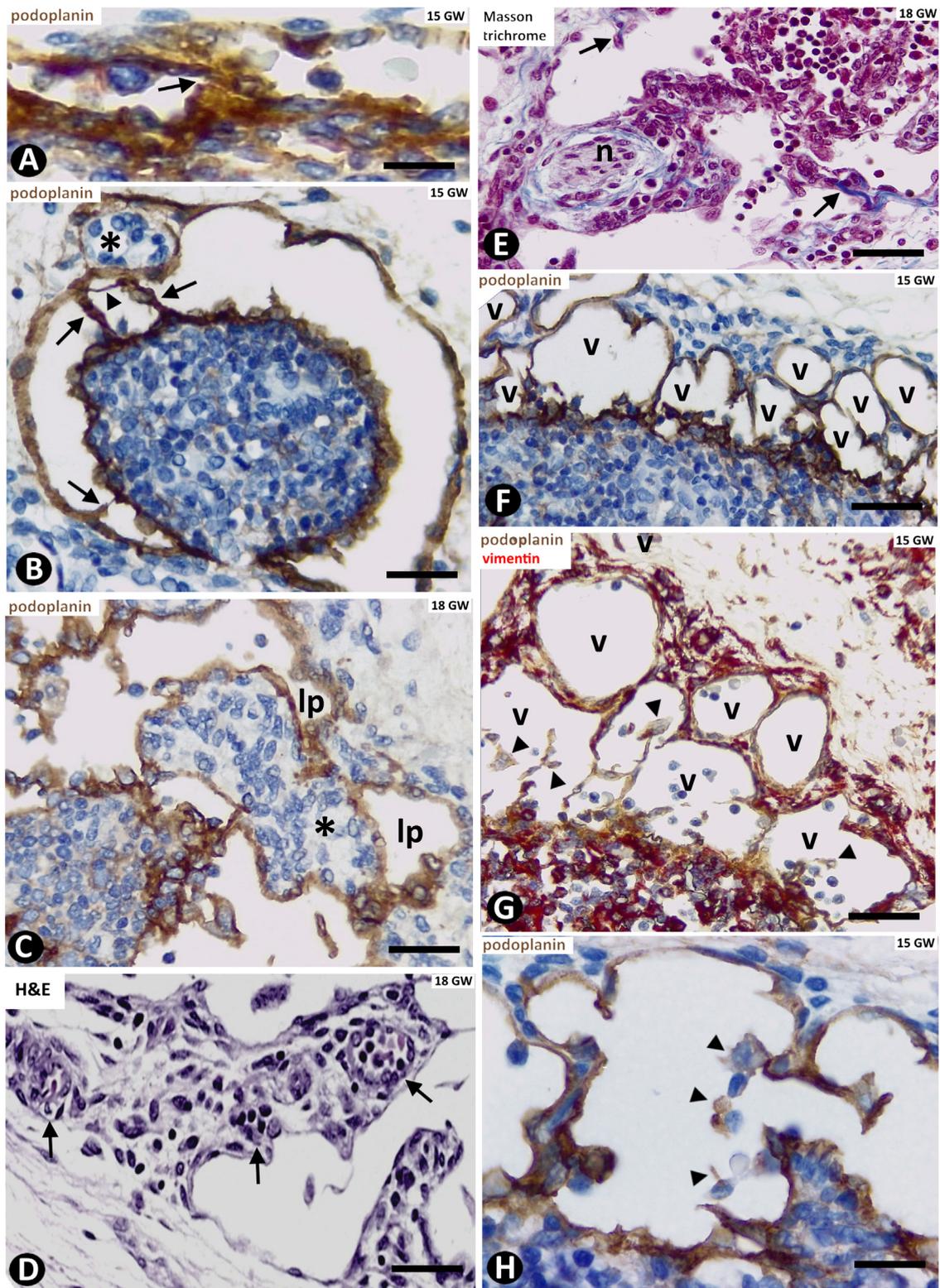
Fig. 5. A to C: Sections immunostained with podoplanin. A: Demonstration of a contact between opposite ceiling and floor LECs (kissing contact, arrow) in a LN sinus. B: One ITS, with scarce prominence in the lumen of the sinus is observed (asterisk). Note that the surrounding LECs form a loop with a virtual lumen. Pillars (arrows) are also present, one of them originating from the same site as the ITS and joined to another pillar by a LEC process (arrowhead). C: ITS (asterisk) partially detached from the LN capsule by a loop (bilaminar sheet) (lp) lined by podoplanin⁺ LECs is observed. Note that the loop lumen differs in size and is also zonally virtual. The internal LEC sheet layer partially covers the ITS, and the external LEC sheet layer lines the connective tissue from which the ITS was segregated. D: In one ITS, blood vessels (arrows) are seen penetrating from the interstitial tissue through an ITS zone that remains attached to the capsule (H&E-staining). E: A nerve strand (n) is observed in an ITS of a pancreatic-duodenal LN. In other zones, pillars (arrows) with a collagen core are also present (Trichrome staining). F–H: Lymphatic merged vessels (v) are observed around anlagen using podoplanin staining (F and H) and podoplanin and vimentin staining (G). Pillars apparently formed from these merged walls are seen (G and H, arrowheads). A to E: pancreatic-duodenal LNs. F and H: popliteal LNs. G: mesenteric LN. A, B, F–H: 15 GW; C-E: 18 GW. Bar: A: 10 μm; B, C, E–G: 20 μm; D: 25 μm; H: 15 μm.
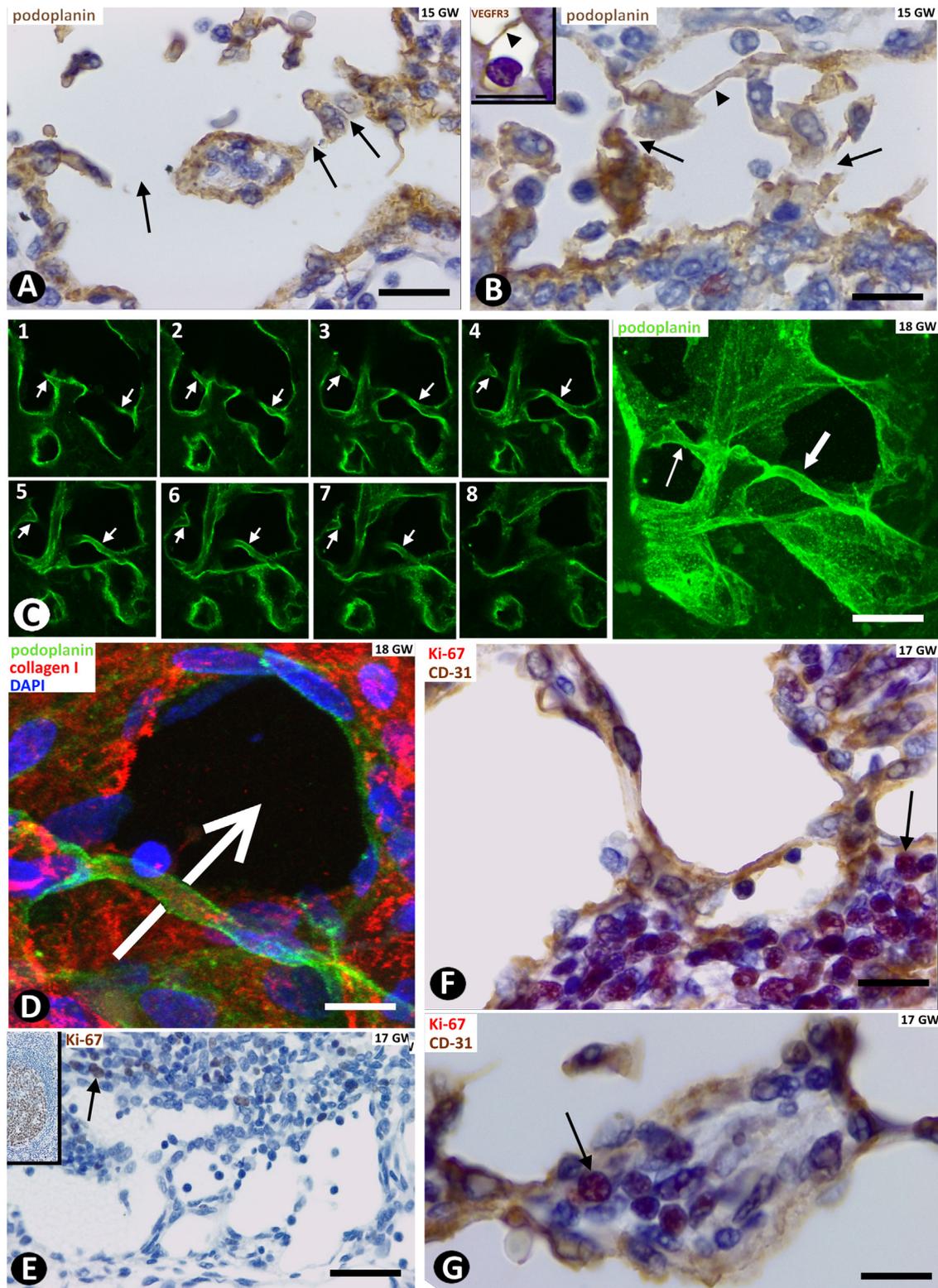
Fig. 6. A and B: Sections immunostained with anti-podoplanin. Vessel intercommunications (arrows) are observed through the spaces formed between the pillars (arrowheads) and the remaining zones of lymphatic merged walls. Note projections of LECs (nascent pillars) joining these structures (B, arrowhead). In the insert of B, a thin LEC projection with VEGFR3 expression is demonstrated (arrowhead). C: Single (1–8) and whole-mount (9) in frontal view (6 μm): podoplanin (green); arrows indicate spatial path of pillars. D: Detail of the whole-mounted intrasinusal pillar indicated in C (thick arrow), now immunostained with podoplanin (green), collagen I (red) and DAPI (blue). The arrow path illustrates the luminal communicating space under the pillar. Note the cover of the pillar formed by LECs and collagen I in the core. E–G: Absence of mitoses and of nuclear expression of Ki-67 in LECs. E: Section immunostained with Ki-67, using internal (some non-LECs, arrow, nuclear staining with Ki-67) and external (insert, tonsil) controls. F and G: Sections with double-immunostaining with CD31 (brown) and Ki-67 (red) in which the CD31$^+$ LECs do not show Ki-67 expression, while some non-LECs (nuclear staining in red, arrow) present Ki-67 expression. A and B: mesenteric LNs, insert of B and C to G: pancreatic-duodenal LNs; A,B: 15 GW; Insert of B: 17 GW; C and D: 18 GW, E, F and G: 17 GW. Bar: A, B, F, G and insert of B: 10 μm; C1-8: 30 μm; C9: 15 μm; D: 8 μm; E: 30 μm. (For interpretation of the references to colour in this figure legend, the reader is referred to the web version of this article.)

4.3. Possible mechanisms of pillar, ITS and fold formation, and of lymphatic space segmentation in LN sinuses

Several complementary mechanisms of pillar and ITS formation have been proposed in blood vessels (Burri and Djonov, 2002; Burri et al., 2004). The morphologic events in developing LN sinuses suggest the possible participation of three of these mechanisms, as follows: (1) The main mechanism proposed for pillar formation includes transcapillary interendothelial unions ("kissing contacts"), followed by reorganization of EC junctions and incorporation of interstitial pillar cores (e.g. collagen bundles) (Burri and Tarek, 1990; Burri, 1990, 1992; Burri et al., 2004; Burri and Djonov, 2002; Djonov et al., 2000, 2002, 2003; Patan et al., 2001a,b; Paku et al., 2011). Our observations of contacts between the opposite LECs (kissing contact between ceiling and floor LECs) of the sinuses with successive formation of pillars and the presence of special junctions involved in the tight three-dimensional integration of the LN sinus intraluminal meshwork (Moll et al., 2009) concur with this mechanism in the formation of LN sinus pillars. (2) The participation of loops in the formation of ITSs has also been proposed in blood vessels, including veins of the ovarian pedicle of nude mice after ovariectomy and human colon adenocarcinoma xenograft (Patan et al., 2001a,b), blood vessel tumours and pseudotumours, dilated hemorrhoidal veins (Díaz-Flores et al., 2016, 2018a, 2018b) and rat femoral vein after perivenous PGE2 and glycerol administration (Díaz-Flores et al., 2017a). The findings of this work also suggest this complementary form of intussusception in ITS incorporation in LN sinuses, by which loops and ITSs are interrelated structures, in which a bilayer of endothelial sheets, arising from the ceiling ECs of the sinus wall, dissects perivascular tissue components, which are incorporated into the sinus lumen (surrounded by the internal endothelial side of the bilayer of LECs). For this mechanism of intussusception in blood vessels, the term "piecemeal form" of intussusceptive angiogenesis has been used in experimental conditions and in vascular tumours with high numbers of pillars and ITSs (Díaz-Flores et al., 2016, 2017a, 2018a,b). (3) Another important and probably frequent procedure in blood vessels is the "merging of adjacent capillaries", whose walls give rise to pillars (Burri and Djonov, 2002; Burri et al., 2004). When these pillars separate from the residual contacting walls, the capillaries intercommunicate, forming a common space. In the developing LNs, the presence of merging lymphatic vessels around anlagen, the formation of pillars from the merged walls and the establishment of intercommunications through the spaces formed between the pillars and the remaining zones of the merged walls, also indicate the possible contribution of this mechanism to the intraluminal meshwork.

Molecular signals that participate in the mechanism of in-itself or intussusceptive blood vessel growth are less known than those involved in sprouting angiogenesis. The factors that influence blood vessel intussusceptive angiogenesis include VEGF (Baum et al., 2010; Gianni-Barrera et al., 2013), ephrinB2/EphB4 signalling (regulating non-sprouting angiogenesis by VEGF) (Groppa et al., 2018), inhibition of endoglin (Hlushchuk et al., 2017) and Notch (Dill et al., 2012; Dimova et al., 2013), (leading to intussusceptive angiogenesis), as well as nitric oxide (switching from sprouting angiogenesis to intussusceptive angiogenesis) (Vimalraj et al., 2018). Interestingly, the VEGF dose located in the microenvironment has an important role in intussusception. Thus, the therapeutic overexpression of VEGF in skeletal muscle (in the limited amount of extracellular matrix) blocked the formation of a gradient to induce tip cell migration in blood vessels and, subsequently, sprouting angiogenesis (Gianni-Barrera et al., 2013). In this way, the high expression of VEGF-C by LT_0 cells (Okuda et al., 2007) and the low production of guidance NPR2 by LN LECs (NPR2 promotes VEGF-C-driven LEC sprouting — Xu et al., 2010) suggested a possible molecular mechanism by which a uniformly high production of VEGF-C in LN cells, in the absence of VEGF-C gradient, results in the non-sprouting engulfing of the LN anlage by LECs (Bovay et al., 2018). This molecular mechanism could also occur in the intussusceptive formation of pillars and ITSs in developing LNs. Further studies are required on the factors that may guide these intussusceptive phenomena, including the influence of other markers (Hoorweg et al., 2015) and biomechanical forces (Bovay et al., 2018).

5. Conclusion

In these immunohistochemical studies of developing foetal LNs using serial histologic sections and confocal microscopy, the results reveal intrasinusal formation of pillars, ITSs and folds, thereby supporting intussusceptive lymphangiogenesis. Consequently, a new role is given to vessel intussusception: participation in the formation of the meshwork of intraluminal processes in LN sinuses, with a known important immunological function. Further studies are required on the factors that regulate lymphatic intussusception.

Ethical statement

Ethical approval for this study was obtained from the Ethics Committee of La Laguna University (CEIBA2018-0322).

References

Bailey, R.P., Weiss, L., 1975. Light and electron microscopic studies of postcapillary venules in developing human fetal lymph nodes. Am. J. Anat. 143, 43–58.

Baum, O., Suter, F., Gerber, B., Tschanz, S.A., Buergy, R., Blank, F., Hlushchuk, R., Djonov, V., 2010. VEGF-A promotes intussusceptive angiogenesis in the developing chicken chorioallantoic membrane. Microcirculation 17, 447–457.

Bénézech, C., White, A., Mader, E., Serre, K., Parnell, S., Pfeffer, K., Ware, C.F., Anderson, G., Caamaño, J.H., 2010. Ontogeny of stromal organizer cells during lymph node development. J. Immunol. 184, 4521–4530.

Bénézech, C., Nayar, S., Finney, B.A., Withers, D.R., Lowe, K., Desanti, G.E., Marriott, C.L., Watson, S.P., Caamaño, J.H., Buckley, C.D., Barone, F., 2014. CLEC-2 is required for development and maintenance of lymph nodes. Blood 123, 3200–3207.

Bovay, E., Sabine, A., Prat-Luri, B., Kim, S., Son, K., Willrodt, A.H., Olsson, C., Halin, C., Kiefer, F., Betsholtz, C., Jeon, N.L., Luther, S.A., Petrova, T.V., 2018. Multiple roles of lymphatic vessels in peripheral lymph node development. J. Exp. Med. 215, 2760–2777.

Burri, P.H., Djonov, V., 2002. Intussusceptive angiogenesis — the alternative to capillary sprouting. Mol. Aspects Med. 23, S1–S27.

Burri, P.H., Tarek, M.R., 1990. A novel mechanism of capillary growth in the rat pulmonary microcirculation. Anat. Rec. 228, 35–45.

Burri, P.H., 1990. Development and growth of the respiratory system. Arch. Int. Physiol. Biochim. 98, A109–A111.

Burri, P.H., 1992. Intussusceptive microvascular growth, a new mechanism of capillary network formation. EXS 61, 32–39.

Burri, P.H., Hlushchuk, R., Djonov, V., 2004. Intussusceptive angiogenesis: its emergence, its characteristics, and its significance. Dev. Dyn. 231, 474–488.

De Spiegelaere, W., Casteleyn, C., Van den Broeck, W., Plendl, J., Bahramsoltani, M., Simoens, P., Djonov, V., Cornillie, P., 2012. Intussusceptive angiogenesis: a biologically relevant form of angiogenesis. J. Vasc. Res. 49, 390–404.

Díaz-Flores, L., Gutiérrez, R., Madrid, J.F., García-Suárez, M.P., González-Álvarez, M.P., Díaz-Flores Jr., L., Sáez, F.J., 2016. Intravascular papillary endothelial hyperplasia (IPEH). Evidence supporting a piecemeal mode of angiogenesis from vein endothelium, with vein wall neovascularization and papillary formation. Histol. Histopathol. 31, 1271–1279.

Díaz-Flores, L., Gutiérrez, R., García, M.D.P., Sáez, F.J., Díaz-Flores Jr., L., Madrid, J.F., 2017a. Piecemeal mechanism combining sprouting and intussusceptive angiogenesis in intravenous papillary formation induced by PGE2 and glycerol. Anat. Rec. (Hoboken) 300, 1781–1792.

Díaz-Flores, L., Gutiérrez, R., García-Suárez, M.P., Sáez, F.J., Gutiérrez, E., Valladares, F., Carrasco, J.L., Díaz-Flores Jr., L., Madrid, J.F., 2017b. Morphofunctional basis of the different types of angiogenesis and formation of postnatal angiogenesis-related secondary structures. Histol. Histopathol. 32, 1239–1279.

Díaz-Flores, L., Gutiérrez, R., González-Gómez, M., García, P., Sáez, F.J., Díaz-Flores Jr., L., Carrasco, J.L., Madrid, J.F., 2018a. Segmentation of dilated hemorrhoidal veins in hemorrhoidal disease. Cells Tissues Organs 205, 120–128.

Díaz-Flores, L., Gutiérrez, R., García, M.ª.P., González-Gómez, M., Sáez, F.J., Díaz-Flores Jr., L., Carrasco, J.L., Madrid, J.F., 2018b. Sinusoidal hemangioma and intravascular papillary endothelial hyperplasia: interrelated processes that share a histogenetic piecemeal angiogenic mechanism. Acta Histochem. 120, 255–262.

Díaz-Flores, L., Gutiérrez, R., García, M.P., González-Gómez, M., Díaz-Flores Jr., L., Carrasco, J.L., Álvarez-Argüelles, H., 2019. Intussusceptive lymphangiogenesis in vascular transformation of lymph node sinuses. Acta Histochem., http://dx.doi.org/10.1016/j.acthis.2019.03.001, Mar 5. pii: S0065-1281(18)30368-4.

Dill, M.T., Rothweiler, S., Djonov, V., Hlushchuk, R., Tornillo, L., Terracciano, L., Meili-Butz, S., Radtke, F., Heim, M.H., Semela, D., 2012. Disruption of Notch1 induces vascular remodeling, intussusceptive angiogenesis, and angiosarcomas in livers of mice. Gastroenterology 142, 967–977, e2.

Dimova, I., Hlushchuk, R., Makanya, A., Styp-Rekowska, B., Ceausu, A., Flueckiger, S., Lang, S., Semela, D., Le Noble, F., Chatterjee, S., Djonov, V., 2013. Inhibition of Notch signaling induces extensive intussusceptive neo-angiogenesis by recruitment of mononuclear cells. Angiogenesis 16, 921–937.

Djonov, V., Schmid, M., Tschanz, S.A., Burri, P.H., 2000. Intussusceptive angiogenesis: its role in embryonic vascular network formation. Circ. Res. 86, 286–292.

Djonov, V.G., Kurz, H., Burri, P.H., 2002. Optimality in the developing vascular system: branching remodeling by means of intussusception as an efficient adaptation mechanism. Dev. Dyn. 224, 391–402.

Djonov, V., Baum, O., Burri, P.H., 2003. Vascular remodeling by intussusceptive angiogenesis. Cell Tissue Res. 314, 107–117.

Eikelenboom, P., Nassy, J.J., Post, J., Versteeg, J.C., Langevoort, H.L., 1978. The histogenesis of lymph nodes in rat and rabbit. Anat. Rec. 190, 201–215.

Gianni-Barrera, R., Trani, M., Fontanellaz, C., Heberer, M., Djonov, V., Hlushchuk, R., Banfi, A., 2013. VEGF over-expression in skeletal muscle induces angiogenesis by intussusception rather than sprouting. Angiogenesis 16, 123–136.

Groppa, E., Brkic, S., Uccelli, A., Wirth, G., Korpisalo-Pirinen, P., Filippova, M., Dasen, B., Sacchi, V., Muraro, M.G., Trani, M., Reginato, S., Gianni-Barrera, R., Ylä-Herttuala, S., Banfi, A., 2018. EphrinB2/EphB4 signaling regulates non-sprouting angiogenesis by VEGF. EMBO Rep. 19, e45054.

Hlushchuk, R., Styp-Rekowska, B., Dzambazi, J., Wnuk, M., Huynh-Do, U., Makanya, A., Djonov, V., 2017. Endoglin inhibition leads to intussusceptive angiogenesis via activation of factors related to COUP-TFII signaling pathway. PLoS One 12, e0182813.

Hoorweg, K., Narang, P., Li, Z., Thuery, A., Papazian, N., Withers, D.R., Coles, M.C., Cupedo, T., 2015. A stromal cell niche for human and mouse type 3 innate lymphoid cells. J. Immunol. 195, 4257–4263.

Lee, Y.G., Koh, G.Y., 2016. Coordinated lymphangiogenesis is critical in lymph node development and maturation. Dev. Dyn. 245, 1189–1197.

Mebius, R.E., 2003. Organogenesis of lymphoid tissues. Nat. Rev. Immunol. 3, 292–303.

Mentzer, S.J., Konerding, M.A., 2014. Intussusceptive angiogenesis: expansion and remodeling of microvascular networks. Angiogenesis 17, 499–509.

Moll, R., Sievers, E., Hämmerling, B., Schmidt, A., Barth, M., Kuhn, C., Grund, C., Hofmann, I., Franke, W.W., 2009. Endothelial and virgultar cell formations in the mammalian lymph node sinus: endothelial differentiation morphotypes characterized by a special kind of junction (complexus adhaerens). Cell Tissue Res. 335, 109–141.

Onder, L., Mörbe, U., Pikor, N., Novkovic, M., Cheng, H.W., Hehlgans, T., Pfeffer, K., Becher, B., Waisman, A., Rülicke, T., Gommerman, J., Mueller, C.G., Sawa, S., Scandella, E., Ludewig, B., 2017. Lymphatic endothelial cells control initiation of lymph node organogenesis. Immunity 47, 80–92, e4.

Okuda, M., Togawa, A., Wada, H., Nishikawa, S., 2007. Distinct activities of stromal cells involved in the organogenesis of lymph nodes and Peyer's patches. J. Immunol. 179, 804–811.

Paku, S., Dezso, K., Bugyik, E., Tóvári, J., Tímár, J., Nagy, P., Laszlo, V., Klepetko, W., Döme, B., 2011. A new mechanism for pillar formation during tumor-induced intussusceptive angiogenesis: inverse sprouting. Am. J. Pathol. 179, 1573–1585.

Patan, S., Alvarez, M.J., Schittny, J.C., Burri, P.H., 1992. Intussusceptive microvascular growth: a common alternative to capillary sprouting. Arch. Histol. Cytol. 55, S65–S75.

Patan, S., Haenni, B., Burri, P.H., 1993. Evidence for intussusceptive capillary growth in the chicken chorio-allantoic membrane (CAM). Anat. Embryol. (Berl). 187, 121–130.

Patan, S., Munn, L.L., Jain, R.K., 1996. Intussusceptive microvascular growth in a human colon adenocarcinoma xenograft: a novel mechanism of tumor angiogenesis. Microvasc. Res. 51, 260–272.

Patan, S., Haenni, B., Burri, P.H., 1997. Implementation of intussusceptive microvascular growth in the chicken chorioallantoic membrane (CAM). Microvasc. Res. 53, 33–52.

Patan, S., Munn, L.L., Tanda, S., Roberge, S., Jain, R.K., Jones, R.C., 2001a. Vascular morphogenesis and remodeling in a model of tissue repair: blood vessel formation and growth in the ovarian pedicle after ovariectomy. Circ. Res. 89, 723–731.

Patan, S., Tanda, S., Roberge, S., Jones, R.C., Jain, R.K., Munn, L.L., 2001b. Vascular morphogenesis and remodeling in a human tumor xenograft: blood vessel formation and growth after ovariectomy and tumor implantation. Circ. Res. 89, 732–739.

Patan, S., 2008. Lycat and cloche at the switch between blood vessel growth and differentiation? Circ. Res. 102, 1005–1007.

Ribatti, D., Djonov, V., 2012. Intussusceptive microvascular growth in tumors. Cancer Lett. 316, 126–131.

van de Pavert, S.A., Mebius, R.E., 2014. Development of secondary lymphoid organs in relation to lymphatic vasculature. In: Kiefer, F., Schulte-Merker, S. (Eds.), Developmental Aspects of the Lymphatic Vascular System. Advances in Anatomy, Embriology and Cell Biology, 214, pp. 81–91.

Vimalraj, S., Bhuvaneswari, S., Lakshmikirupa, S., Jyothsna, G., Chatterjee, S., 2018. Nitric oxide signaling regulates tumor-induced intussusceptive-like angiogenesis. Microvasc. Res. 119, 47–59.

Vondenhoff, M.F., van de Pavert, S.A., Dillard, M.E., Greuter, M., Goverse, G., Oliver, G., Mebius, R.E., 2009a. Lymph sacs are not required for the initiation of lymph node formation. Development 136, 29–34.

Vondenhoff, M.F., Greuter, M., Goverse, G., Elewaut, D., Dewint, P., Ware, C.F., Hoorweg, K., Kraal, G., Mebius, R.E., 2009b. LTbetaR signaling induces cytokine expression and up-regulates lymphangiogenic factors in lymph node anlagen. J. Immunol. 182, 5439–5445.

Wang, Z., Chai, Q., Zhu, M., 2018. Differential roles of LTβR in endothelial cell subsets for lymph node organogenesis and maturation. J. Immunol. 201, 69–76.

Willard-Mack, C.L., 2006. Normal structure, function, and histology of lymph nodes. Toxicol. Pathol. 34, 409–424.

Xu, Y., Yuan, L., Mak, J., Pardanaud, L., Caunt, M., Kasman, I., Larrivée, B., Del Toro, R., Suchting, S., Medvinsky, A., Silva, J., Yang, J., Thomas, J.L., Koch, A.W., Alitalo, K., Eichmann, A., Bagri, A., 2010. Neuropilin-2 mediates VEGF-C-induced lymphatic sprouting together with VEGFR3. J. Cell Biol. 188, 115–130.